Short Papers

An Analysis of a Waveguide T Junction with an Inductive Post

Jiro Hirokawa, Kimio Sakurai, Makoto Ando, and Naohisa Goto

Abstract—**The authors analyze the T junction with an inductive post taking its diameter into account for the case where the current distribution is assumed on the surface of the post. A single cylindrical post placed in a T junction improves the impedance matching and compensates the junction discontinuity in a wide frequency band. The analysis clarifies the effects of the design parameters such as the diameter of the post and its location. It accurately predicts the measured return loss. On the basis of this analysis, an effective design procedure of the T junction is proposed and the reflection below −30 dB is realized over 4% bandwidth.**

I. Introduction

Slotted waveguide arrays are free of conductor loss and are promising candidates for high-gain and high-efficiency planar antennas. Various kinds have been developed for the application of DBS (direct broadcasting from satellite) reception [1], [2]. The serious difficulty of this antenna is its relatively high cost in mass production. In particular, a feeding structure suitable for manufacturing is highly desired. The authors had proposed a single-layer slotted waveguide array [2] in which a simple feeding waveguide is placed on the same layer of the radiating waveguides, as in Fig. 1. The coupling windows are cut on the narrow wall of the feeding waveguide. In order to cover the DBS bandwidth from 11.7 to 12.0 GHz in Japan, the long line effects must be suppressed by reducing the number of coupling windows in one feeding waveguide. To realize a sufficiently large antenna aperture, these units may be collinearly arrayed and excited by another corporate-feed waveguide as is shown in Fig. 1. A two-way power divider is the key component in this system. A waveguide T junction with an inductive post is attractive from a manufacturing point of view [3].

This paper presents the analysis and the design of a waveguide T junction with an inductive post for use as a two-way power divider in a slotted waveguide array feed. A single cylindrical post, placed across the waveguide parallel to the narrow walls of a waveguide, suppresses reflection in a wide frequency band. The power handling capability of this structure is excellent since there is no gap where the electric field is concentrated.

In Section II we analyze the fields in the T junction with an inductive post using the method of moments. The problem is two-dimensional. Special attention is paid to evaluate the effects of the post diameter, and the current distribution on the surface of the post is expanded in a series. The effects of the design parameters upon the reflection and transmission through the T junction are discussed in Section III. The experiments confirm the prediction of the reflection for various diameters and locations of the post. In Section IV we propose an effective design procedure for the T junction with an inductive post.

Manuscript received April 17, 1990; revised October 21, 1990. This work was supported in part by a Scientific Grant-in-Aid (63420032) from the Ministry of Education, Science and Culture in Japan.

The authors are with the Department of Electrical and Electronic Engineering, Faculty of Engineering, Tokyo Institute of Technology, Oookayama, Meguro-ku, Tokyo 152 Japan.

IEEE Log Number 9041962.

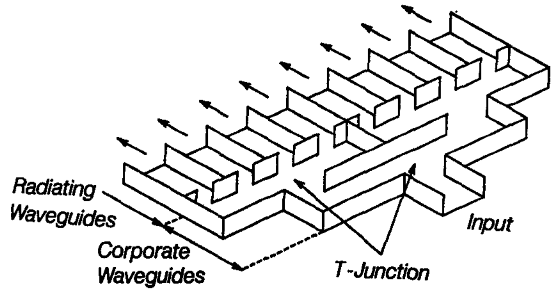

Fig. 1. A single-layer slotted waveguide array.

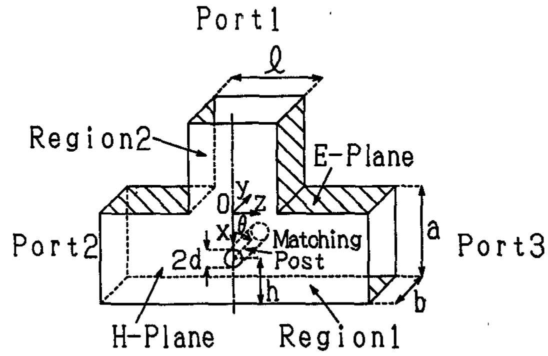

Fig. 2. Waveguide T junction with an inductive post.

II. Analysis

The configuration of the T junction with an inductive post is shown in Fig. 2, together with its coordinate system. The widths of two waveguides are a and l, and the common height is b. The post is located at $x = a - h$ and $z = 0$. The diameter of the post is $2d$. Let a TE_{10} to x mode of unit amplitude be incident on the aperture of the T junction from port 1, as in Fig. 2. Since the incident wave as well as the structure of the T junction is uniform in the y direction, the total field in the T junction does not vary in the y direction [4]. The problem is then a two-dimensional one.

The field equivalent theorem enables us to reduce the T junction into two simple regions, as in Fig. 3. Then, the field in each region is expressed by using the dyadic Green's function in a rectangular waveguide. An unknown electric current distribution J is assumed on the surface of the post S_1. According to the field equivalence theorem, the aperture S_2 is replaced by an unknown equivalent magnetic current $\boldsymbol{M}$. The continuity conditions for the tangential electric field on S_1 and that for the

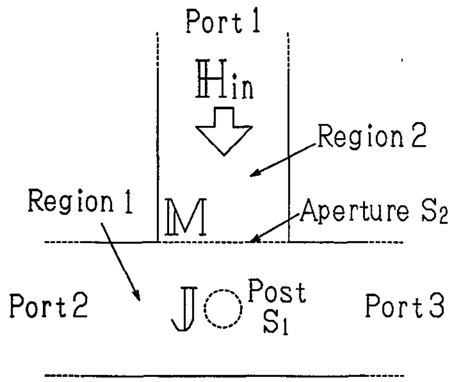

Fig. 3. Unknown electric and magnetic currents.

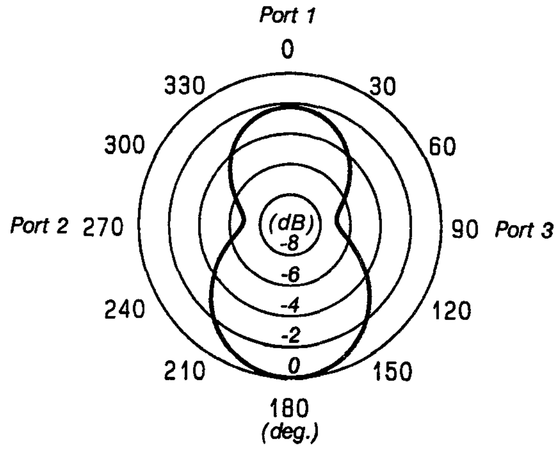

Fig. 4. Calculated current distribution on the post (position $h = 25.5$ mm; diameter $2d = 4.0$ mm).

tangential magnetic field on S_2 require a set of integral equations, (1) and (2), for unknown currents $\boldsymbol{J}$ and $\boldsymbol{M}$.

On S_1,

$$\iint_{S_1} \overline{\overline{G^e_{1e}}} \cdot \boldsymbol{J} ds + \iint_{S_2} \overline{\overline{G^e_{1m}}} \cdot \boldsymbol{M} ds = \boldsymbol{O}. \tag{1}$$

On S_2,

$$\iint_{S_1} \overline{\overline{G^m_{1e}}} \cdot \boldsymbol{J} ds + \iint_{S_2} \overline{\overline{G^m_{1m}}} \cdot \boldsymbol{M} ds = -\iint_{S_2} \overline{\overline{G^m_{2m}}} \cdot \boldsymbol{M} ds + \boldsymbol{H}_{\text{in}} \tag{2}$$

where $\boldsymbol{H}_{\text{in}}$ is the tangential component of the magnetic field (TE_{10} mode) incident from the port 1. The $\overline{\overline{G}}$'s are the usual dyadic Green's functions in rectangular waveguides [5]:

- $\overline{\overline{G^e_{1e}}}$: For the electric field produced by a unit electric current in the region 1.
- $\overline{\overline{G^e_{1m}}}$: For the electric field produced by a unit magnetic current in the region 1.
- $\overline{\overline{G^m_{1e}}}$: For the magnetic field produced by a unit electric current in the region 1.
- $\overline{\overline{G^m_{km}}}$: For the magnetic field produced by a unit magnetic current in the region k $(k = 1, 2)$.

These dyadic Green's functions are expanded in terms of a complete set of the normal mode function TE_{n0} which does not vary with y.

For the reduction of (1) and (2) to a system of linear equations, Galerkin's method of moments is adopted. An unknown electric current on the post $\boldsymbol{J}$ has only a y component, which does not vary with y since only the TE_{n0} modes exists in the waveguide. For the same reason, an unknown magnetic current on the aperture $\boldsymbol{M}$ has only a z component. $\boldsymbol{J}$ and $\boldsymbol{M}$ are expanded by basis functions which reflect the symmetrical structure of the T junction:

$$\boldsymbol{J} = \hat{\boldsymbol{y}} \sum_{m_j} A_{mj} \frac{Y_0}{2\pi d} \cos(m_j \theta) = \sum_{m_j} A_{mj} \boldsymbol{j}_{mj} \qquad (m_j = 0, 1, 2, \cdots) \tag{3}$$

$$\boldsymbol{M} = \hat{\boldsymbol{z}} \sum_{n_j} \left(\frac{2}{lb} \right)^{1/2} \cos \frac{n_j \pi z}{l} = \sum_{nj} B_{nj} \boldsymbol{m}_{nj} \qquad (n_j = 1, 3, 5, \cdots) \tag{4}$$

where the A_{mj} and B_{nj} are the unknown expansion coefficients of $\boldsymbol{J}$ and $\boldsymbol{M}$, respectively. Y_0 is the characteristic admittance in free space. Equations (3) and (4) are substituted into (1) and (2). Then (1) is multiplied by the basis function $\boldsymbol{j}_{mi}$ of $\boldsymbol{J}$ and is integrated over the surface of the post S_1. On the other hand, (2) is multiplied by the basis function $\boldsymbol{m}_{ni}$ of $\boldsymbol{M}$ and is integrated over the aperture S_2. As a result, a system of linear equations, (5) and (6), for A_{mj} and B_{nj} is obtained:

$$\sum_{mj} A_{mj} \iint_{S_1} \iint_{S_1} \boldsymbol{j}_{mi} \cdot \overline{\overline{G^e_{1e}}} \cdot \boldsymbol{j}_{mj} \, ds_j \, ds_i + \sum_{nj} B_{nj} \iint_{S_1} \iint_{S_2} \boldsymbol{j}_{mi} \cdot \overline{\overline{G^e_{1m}}} \cdot \boldsymbol{m}_{nj} \, ds_j \, ds_i = 0 \tag{5}$$

$$\sum_{mj} A_{mj} \iint_{S_2} \iint_{S_1} \boldsymbol{m}_{ni} \cdot \overline{\overline{G^m_{1e}}} \cdot \boldsymbol{j}_{mj} \, ds_j \, ds_i + \sum_{nj} B_{nj} \iint_{S_2} \iint_{S_2} \boldsymbol{m}_{ni} \cdot \left(\overline{\overline{G^m_{1m}}} + \overline{\overline{G^m_{2m}}} \right) \cdot \boldsymbol{m}_{nj} \, ds_j \, ds_i = \iint_{S_2} \boldsymbol{m}_{ni} \cdot \boldsymbol{H}_{\text{in}} \, ds_i. \tag{6}$$

Once (5) and (6) are solved for A_{mj} and B_{nj}, $\boldsymbol{J}$ and $\boldsymbol{M}$ are determined from (3) and (4) [6].

The reflection power to port 1 is calculated as the sum of the reflecting wave of the incident wave $\boldsymbol{H}_{\text{in}}$ and the scattering wave by the magnetic current $\boldsymbol{M}$ on the aperture. The transmission powers to ports 2 and 3 are calculated as the scattering wave by the electric current $\boldsymbol{J}$ on the post and the magnetic current $\boldsymbol{M}$ on the aperture [5].

III. Numerical Results and Measurement

A standard waveguide for 4 GHz band is used to make a scale model of the T junction. The width of the broad wall of a waveguide is 58.1 mm. The design frequency is 3.95 GHz, which is one third of 11.85 GHz, the center frequency of the DBS band in Japan. In experiments, the reflection and transmission coefficients are measured between the two ports, with the other port terminated by a matched load whose reflection is below -40 dB. We have confirmed by measurements that the power from port 1 is divided equally between ports 2 and 3.

Fig. 4 is an example of the calculated current distribution on the surface of the post. The current density varies on the surface considerably. This suggests the importance of the higher modes of the electric current $\boldsymbol{J}$ on the post. On the other hand, the next higher mode ($n_j = 3$ in (4)) of the magnetic current $\boldsymbol{M}$ on the aperture S_2 is less than -20 dB of the first-order mode ($n_j = 1$ in (4)) and can be ignored in the analysis.

To grasp the effects of the diameter and the location of the post, reflection is calculated for a wide variety of parameters. Fig. 5 shows the contour map of the reflection as functions of

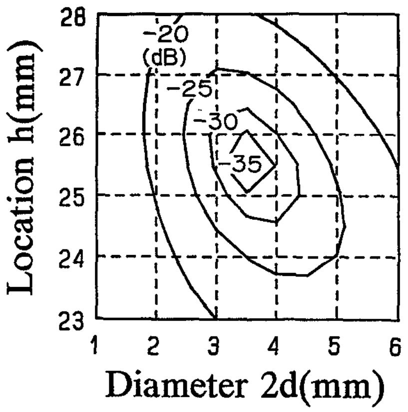

Fig. 5. Contour map of calculated reflection at 3.95 GHz.

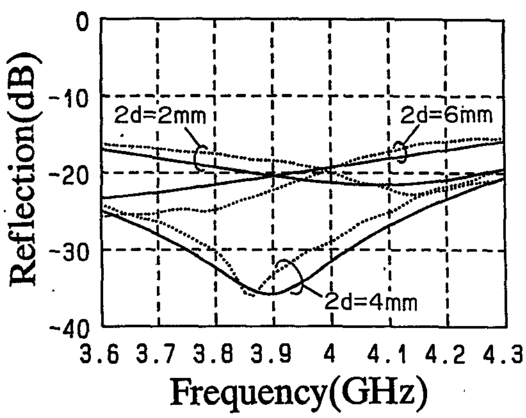

Fig. 6. Frequency characteristics of reflection for various diameters of the post. (——— calculated; · · · · measured).

the diameter of the post $2d$ and its location h: the ratio of the reflection power to the incident power at port 1 is indicted in the figure. The minimum reflection is obtained for $h = 25.5$ mm and $2d = 3.5$ mm. The contour of the equal reflection is elliptical: the reflection is more sensitive to the parameter $2d$ than to the parameter h. For example, for $2d = 3.5$ mm, the reflection below -30 dB is realized in the range $h = 24.6$ mm ~ 26.4 mm. On the other hand, for $h = 25.5$ mm, the same level is realized in the narrower range $2d = 3.0$ mm ~ 4.2 mm.

Fig. 6 shows the predicted and measured frequency characteristics of the reflection for $2d = 2$, 4, and 6 mm and $h = 25.5$ mm. The analysis reasonably predicts the measured dependence of the reflection upon the diameter of the post $2d$. For $2d = 4$ mm, the measured reflection is below -30 dB from 3.80 GHz to 3.96 GHz (4.1% bandwidth). This characteristic is sufficient for the power divider of the DBS antennas (2.5% bandwidth in Japan). The diameter is almost optimum in terms of reflection suppression. For a diameter $2d$ different from the optimum one, the reflection gets larger and its minimum also grows.

Fig. 7 shows the calculated and measured frequency characteristics of the reflection for $h = 23.5$, 25.5, and 27.5 mm and $2d = 4$ mm. The analysis accurately predicts the experimental reflection for various locations of the post h. For a given location h, there exists some frequency for which the reflection below -30 dB is realized.

Good agreement between the calculated result and the measured one verifies our analysis. The optimum configuration of the T junction has an excellent characteristic: the reflection below -30 dB is realized over 4.1% frequency bandwidth.

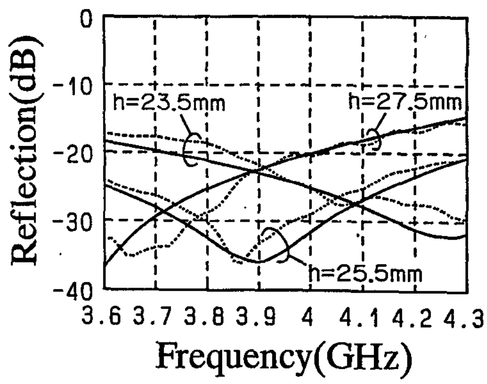

Fig. 7. Frequency characteristics of reflection for various locations of the post (——— calculated; · · · · measured).

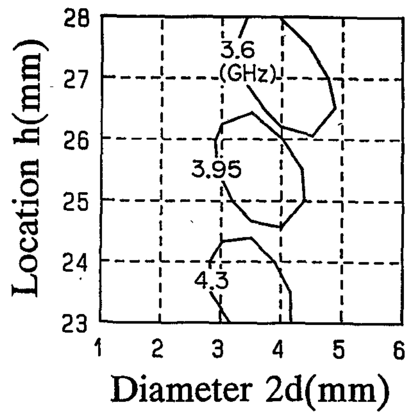

Fig. 8. Contour map of calculated reflection below -30 dB.

IV. Design

In this section, a noniterative design procedure for the T junction with an inductive post is proposed. Fig. 8 shows the contour map of the reflection below -30 dB as a function of the diameter of the post $2d$ and the location h at frequencies of 3.6 GHz, 3.95 GHz, and 4.3 GHz. As the frequency gets higher, the optimum value of the location h_{opt} gets smaller. It is noted that h_{opt} is about one fourth of the guide wavelength in each frequency. On the other hand, the optimum diameter is almost independent of the frequency ($2d_{opt} = 3.5 \sim 4.0$ mm).

On the basis of these numerical results, the following straightforward procedures are recommended for the design of a T junction with an inductive post.

1) The diameter of the post, $2d$, is optimized to reduce the reflection. In this procedure 1/4 guide wavelength provides a suitable initial value for the location of the post h. Only the minimum value of reflection should be pursued and the optimum frequency may be different from the design.
2) The location of the post h is optimized to shift the optimum frequency to the design one. In this step, the reflection level remains small and only a shift in frequency is expected.

V. Conclusion

The authors analyze a waveguide T junction with an inductive post, taking the diameter of the post into account. The analysis clarifies the effects of the parameters. It accurately predicts the measured reflection for various diameters and locations of the post. The diameter of the post is found to be particularly important in realizing sufficiently small reflection. On the basis of the analysis, the location and the diameter of the post are optimized: reflection below −30dB is realized over a 4% bandwidth. A noniterative procedure is proposed for the general design of the T junction.

Acknowledgment

The authors are deeply indebted to Dr. K. Hirasawa (Associate Professor, University of Tsukuba), Dr. H. Arai (Lecturer, Yokohama National University), Dr. H. Seki (Associate Professor, Nagaoka University of Technology), Dr. H. Mizuno, and Dr. T. Nomoto (NHK Science and Technical Research Laboratory) for their fruitful advice. Thanks are also due to K. Maehara (Asahi Chemical Industry Co. Ltd.), who gave us advice from a manufacturing view point.

References

[1] J. Takada, M. Ando, and N. Goto, "A slot coupling control in circularly-polarized radial line slot antenna," *1989 IEEE AP-S Int. Symp. Dig.*, vol. 3, June 1989, pp. 1456–1459.

[2] N. Goto, "A waveguide-fed printed antenna," IEICE Japan. Tech. Rep. AP89-3, Apr. 1989.

[3] H. Mizuno, T. Nomoto, and H. Mitsumoto, "A 4-way power divider using *E*-plane circular bend structure," in *Conf. Rec., Nat. Conv.*, C-788, IEICE Japan, Mar. 1989.

[4] Y. Leviatan, P. G. Li, A. T. Adams, and J. Perini, "Single-post inductive obstacle in rectangular waveguide," *IEEE Trans. Microwave Theory Tech.*, vol. MTT-31, pp. 806–812, Oct. 1983.

[5] R. E. Collin, *Field Theory of Guided Waves*. New York: McGraw-Hill, 1960.

[6] H. Seki, "An alternative representation of electromagnetic fields in a rectangular waveguide with an aperture in its wall." in *Conf. Rec., Nat. Conv.*, 16, IEICE Japan, Sept. 1984, p. 16.

A Theoretical Examination of Tangential Signal to Noise Ratio

Harry E. Green

Abstract **—The tangential signal to noise ratio (TSNR) continues to be used as a measure of receiver sensitivity. It is found in practice to be remarkably robust against a variety of equipment and observers. Based on the physiology of the eye, an explanation of why this is so is given in this note. The theory leads to a result for TSNR which is very close to the generally agreed value.**

I. Introduction

A measure of receiver system sensitivity which dates from the early days of radar is the tangential signal to noise (TSNR). The term continues to be used in technical data; e.g., diodes used in direct detection receivers are commonly characterized in terms of TSNR in manufacturers' catalogs.

When one looks at an A-scope in which signals in the form of rectangular pulses are present together with noise, the display has something of the appearance shown in Fig. 1. Between the pulses there are bands of light produced by the noise having fuzzy but nonetheless discernible edges. At the position of the pulses the noise is lifted up on a pedestal. When the pulse signal power is adjusted so that the lower edge of the noise trace thereon is level or tangential with the upper edge of the noise-only trace, a TSNR is said to have been achieved.

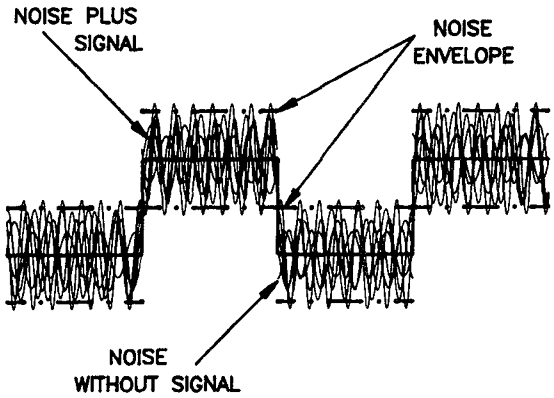

Fig. 1. Signal and noise with a tangential signal to noise ratio.

The advantage of the method, particularly when first devised, is that it can be carried out simply with ready-to-hand apparatus. On the other hand, the very range of possible measuring equipment, the ill-defined experimental conditions, and the physiological variations between observers would lead to an expectation of fairly meaningless results. In practice this turns out not to be the case. Remarkably consistent results are obtained by a range of observers using a variety of equipment.

In this note the reason for this consistency is investigated. Based on measurements made by various observers, it seems generally agreed that TSNR corresponds to a signal to noise ratio of about 8 dB [1]–[3]. A figure very close to this results from the simple theoretical considerations presented herein.

II. Theoretical Development

The human eye has a resolving power of around one minute of arc and the minimum viewing distance which produces no fatigue is about 450 mm [4]. At this range there will therefore be about 8 pixels/mm and a typical laboratory CRO screen will divide vertically into about 1000 pixel width strips (PWS's).

Imagine that we are viewing baseband noise band limited in B. Suppose that we divide each PWS into the vertical stack of pixels suggested in Fig. 2. If as the strobe passes through each PWS light is to be emitted essentially from a single pixel, then we require that the time of passage of the beam be small compared with the correlation time of the noise [5], i.e., $f_s \gg 0.001B$, where f_s is the strobe frequency (sweeps/s). On the other hand, if within a given PWS pixels painted in successive passes are to be statistically independent, the strobe period must be long compared with the correlation time, i.e., $f_s \ll B$. It is obvious that both constraints can be satisfied simultaneously with a large range of strobe frequencies.

The noise is assumed zero mean Gaussian with pdf

$$p(y) = \left(1/\sqrt{2\pi}\sigma\right)\exp-\left(y^2/2\sigma^2\right) \tag{1}$$

where σ is the rms noise voltage. Suppose that we set the vertical sensitivity of the CRO so that σ corresponds to a beam displacement from the axis of N pixels; i.e., each pixel is of height $\Delta = \sigma/N$. Then the probability that the electron beam

Manuscript received June 5, 1990; revised October 4, 1990.

The author is with the Surveillance Research Laboratory, High Frequency Radar Division, Defence Science & Technology Organisation, Department of Defence, P.O. Box 1650, Salisbury, South Australia, 5108, Australia.

IEEE Log Number 9041937.